Journal of Cell Science 113, 4451-4461 (2000)
Printed in Great Britain © The Company of Biologists Limited 2000
JCS2013

Characterization of the amino-terminal regions in the human multidrug resistance protein (MRP1)

Éva Bakos[1,2,*], Raymond Evers[3,*], Giulia Calenda[3], Gábor E. Tusnády[2], Gergely Szakács[1], András Váradi[2] and Balázs Sarkadi[1,‡]

[1]National Institute of Haematology and Immunology, Research Group of the Hungarian Academy of Sciences, H-1113 Budapest, Hungary
[2]Institute of Enzymology, Biological Research Center, Hungarian Academy of Sciences, H-1113 Budapest, Hungary
[3]Georg-Speyer-Haus, Institute for Biomedical Research, 60596 Frankfurt am Main, Germany
*These authors contributed equally to this work
‡Author for correspondence (e-mail: B.Sarkadi@ohvi.hu)

Accepted 9 October; published on WWW 16 November 2000

SUMMARY

The human multidrug resistance protein (MRP1) contributes to drug resistance in cancer cells. In addition to an MDR1-like core, MRP1 contains an N-terminal membrane-bound (TMD_0) region and a cytoplasmic linker (L_0), both characteristic of several members of the MRP family. In order to study the role of the TMD_0 and L_0 regions, we constructed various truncated and mutated MRP1, and chimeric MRP1-MDR1 molecules, which were expressed in insect (Sf9) and polarized mammalian (MDCKII) cells. The function of the various proteins was examined in isolated membrane vesicles by measuring the transport of leukotriene C_4 and other glutathione conjugates, and by vanadate-dependent nucleotide occlusion. Cellular localization, and glutathione-conjugate and drug transport, were also studied in MDCKII cells. We found that chimeric proteins consisting of N-terminal fragments of MRP1 fused to the N terminus of MDR1 preserved the transport, nucleotide occlusion and apical membrane routing of wild-type MDR1. As shown before, MRP1 without TMD_0L_0 (ΔMRP1), was non-functional and localized intracellularly, so we investigated the coexpression of ΔMRP1 with the isolated L_0 region. Coexpression yielded a functional MRP1 molecule in Sf9 cells and routing to the lateral membrane in MDCKII cells. Interestingly, the L_0 peptide was found to be associated with membranes in Sf9 cells and could only be solubilized by urea or detergent. A 10-amino-acid deletion in a predicted amphipathic region of L_0 abolished its attachment to the membrane and eliminated MRP1 transport function, but did not affect membrane routing. Taken together, these experiments suggest that the L_0 region forms a distinct domain within MRP1, which interacts with hydrophobic membrane regions and with the core region of MRP1.

Key words: Multidrug resistance protein, MRP, Truncated MRP, N-terminal linker region, LTC_4 transport, NEM-GS transport, Nucleotide trapping, Polarized cell

INTRODUCTION

MDR1 Pgp (multidrug transporter P-glycoprotein) and MRP1 (multidrug resistance protein 1) are members of the ABC (ATP-Binding Cassette) transporter family that are able to extrude chemotherapeutic drugs from tumor cells in an ATP-dependent manner. Whereas MDR1 preferentially transports hydrophobic, slightly positive molecules, MRP1 transports glutathione (GS) conjugates (e.g. leukotriene C_4, LTC_4) and other large hydrophobic molecules conjugated to negatively charged ligands like sulfate and glucuronide (Gottesman and Pastan, 1993; Jedlitschky et al., 1996; Jedlitschky et al., 1994; Loe et al., 1996b; McGrath et al., 1989; Muller et al., 1994). MRP1 also transports unmodified neutral and basic organic compounds, probably by a cotransport mechanism together with glutathione (Evers et al., 2000; Loe et al., 1996a; Loe et al., 1998). MDR1 Pgp and MRP1 seem to be major players in chemotherapy resistance in numerous forms of cancer, although homologs of these two transporters, as well as the recently identified breast cancer resistance protein (BCRP/MXR/ABCP) may also be involved in this clinical phenomenon (Doyle et al., 1998).

In connection with its hydrophobic drug transport activity, MDR1 has been shown to possess a drug-stimulated ATPase activity (Sarkadi et al., 1992; Scarborough, 1995). Hydrophobic drug and glutathione-conjugate extrusion by MRP1 is also dependent on the hydrolysis of ATP (Bakos et al., 2000; Chang et al., 1998; Mao et al., 1999). The transport and ATPase cycle of both proteins are inhibited by vanadate, which stabilizes a transition state intermediate of the ATPase cycle, with an occluded nucleotide in the catalytic site. Similar to the ATPase, the rate of the vanadate-dependent nucleotide occlusion is greatly accelerated by the transported substrates (Szabó et al., 1998; Taguchi et al., 1997; Ueda et al., 1997).

MDR1 and MRP1 share a similar core structure, containing a tandem repeat of transmembrane domains (TMDs) and cytoplasmic ATP-binding cassette (ABC) regions. However, MRP1 and several homologues form a subfamily of ABC-transporters, characterized by a triple membrane-bound domain structure. These include an MDR1-like core region, containing two ABC units and two membrane-bound domains (TMD_1 and TMD_2), and an N-terminal polypeptide region of about 280 amino acids, forming a cytoplasmic loop and a membrane-bound domain (L_0 and TMD_0, respectively; see Bakos et al., 1998; Tusnády et al., 1997; Fig. 1A). In polarized cells MDR1 is targeted to the apical membrane, whereas MRP1 is routed to the basolateral membrane (Bakos et al., 1998; Evers et al., 1996).

In our previous studies on the role of the N-terminal regions of MRP1 in the function and plasma membrane targeting of human MRP1, we showed that the MDR1-like core has practically no transport and nucleotide occlusion activity (Bakos et al., 1998). Transport function, however, could be restored by coexpressing the full N-terminal TMD_0L_0 region together with the MDR1-like core region (see also Gao et al., 1998). We also found that extending the core with the N-terminal linker in the absence of the TMD_0 region, resulted in an active transporter that was properly routed to the plasma membrane (Bakos et al., 1998).

Our previous studies indicated that the L_0 region is sufficient and essential for MRP1-mediated transport activity and routing to the lateral membrane in polarized cells. We investigated in this study whether fusing parts of TMD_0L_0 to the N terminus of MDR1 would result in changes in substrate specificity or plasma membrane routing of MRP1-MDR1 chimeras. Furthermore, to investigate whether the L_0 intracellular loop specifically interacts with the core region of MRP1, we coexpressed L_0 with truncated forms of MRP1. Constructs were expressed both in baculovirus infected *Spodoptera frugiperda* ovarian (Sf9) cells and in Madin-Darby canine kidney (MDCKII) cells. We show here that all MRP1-MDR1 chimeric proteins preserved the characteristics of MDR1. However when the truncated MRP1 core was coexpressed with the L_0 peptide, a functional MRP1 molecule was obtained that was localized in the lateral membrane. Our experiments suggest that the intracellular loop L_0 forms a domain that interacts both with hydrophobic membrane regions and, specifically, with the core region of MRP1.

MATERIALS AND METHODS

Generation of MRP1 variants and recombinant baculoviruses

In order to generate the MRP1-MDR1 chimeric constructs, the full-length MDR1 cDNA was cloned into the *Bam*HI site of Bluescript SK. The *Bam*HI-*Eco*RI (nucleotides (nt) –8-1177) fragment was removed from Bluescript-MDR1 and subcloned into M13mp18, and an *Xba*I site was introduced by site-directed mutagenesis at nt 4 of MDR1. The *Xba*I-*Eco*RI fragment from this construct and the *Eco*RI-*Not*I (*Not*I of the polycloning site) fragment from Bluescript-MDR1 were ligated together into the pVL1393 baculovirus transfer vector, yielding pVL1393MDR1. Previously, an *Xba*I site was introduced at nt 606 of the MRP1 cDNA in M13SBMRP1 (Bakos et al., 1998). To obtain TMD_0MDR1 chimeric cDNA, a *Dra*III-*Bam*HI fragment (nt 87-840) was removed from the pAcSG2MRP (Bakos et al., 1998) and replaced by the *Dra*III-*Bam*HI insert of M13SBMRP1. An *Xba*I-*Xba*I fragment (nt –5-606) fragment was subcloned into the *Xba*I site of pVL1393MDR1. To generate the TMD_0L_0MDR1 the pAcSG2MRPlinkerI (Bakos et al., 1998) was digested with *Nhe*I within the linker I preceeding the stop codon and the *Xba*I site at position –5. The fragment was subcloned into the *Xba*I site of pVL1393MDR1. To obtain L_0MDR1, linker I (Bakos et al., 1998) was inserted into the unique *Bam*HI site of the pAcSG2MRPlinkerII. The pAcSG2MRPlinkerII/linkerI was digested with *Nhe*I within linker I and II. The fragment was subcloned into the *Xba*I site of pVL1393MDR1.

The MRP1Δ(223-232) mutant was generated by overlap PCR using pJ3Ω-MRP1 (Zaman et al., 1994) as the template. The following primers were used: 5′gatgtcgacaccggcatggcgctccggggcttc3′ (primer 1; *Sal*I site underlined), 5′cactgccctccaggggctggcgccagaaggtgatcctcg-acagg3′ (primer 2), 5′cctgtcgaggatcaccttctggcgccagcccctggagggcagtg3′ (primer 3, encoding amino acids (aa) 216-222 and 233-239, and complementary to primer 2), 5′ctcctcattcgcatccaccttggaactctc3′ (primer 4, aa 287-297). The upstream fragment was generated using primers 1 and 2, the downstream fragment using primers 3 and 4. Both fragments were gel purified, combined and a PCR reaction with primers 1 and 4 was performed. The amplified overlap product was digested with *Sal*I-*Bam*HI and the fragment was substituted for the original *Sal*I-*Bam*HI fragment in pJ3Ω-MRP1, resulting in pJ3Ω-MRP1(Δ223-232).

To generate the isolated L_0 the pAcSG2MRPlinkerII/linkerI construct was partially digested with *Nhe*I in linker II and *Spe*I in linker I. The fragment (encoding aa MAL+204-281+LLA+Stop) was subcloned into the *Xba*I site of pVL1392. To obtain the L_0Δ(223-232) fragment, the fragment encoding aa 204-281 was amplified by PCR using pJ3ΩMRP1(Δ223-232) as the template. The forward primer used was 5′ taggctagccggcatggaccctaatccctgcccaga3′, the reverse primer used was 5′ cggctagatctaatccttggaggagtacac3′. The primers included *Nhe*I and *Bgl*II sites, respectively. The PCR fragment was digested with *Nhe*I and *Bgl*II and the fragment was cloned into pVL1393. All constructs were verified by sequence analysis.

Sf9 (*Spodoptera frugiperda*) cells were cultured and infected with a baculovirus as described earlier (Sarkadi et al., 1992). Recombinant baculoviruses were generated by using the BaculoGold Transfection Kit (PharMingene).

Generation of MDCKII cells expressing MRP1 variants

For expression of MRP1 variants in MDCKII cells (kindly provided by Dr G. van Meer, Amsterdam, The Netherlands), the L_0MDR1 chimera, ΔMRP1 and MRP1Δ(223-232) were inserted as blunt-end fragments into the retroviral vector pCMV-neo as described (Bakos et al., 1998). For coexpression experiments the L_0 fragment was cloned into the pBabe-Puro-CMV vector (kindly provided by Dr J. Wijnholds, The Netherlands Cancer Institute, Amsterdam, The Netherlands). This vector was generated by cloning the blunt-ended *Hin*dIII fragment from pCMV-neo (containing the CMV early promoter) into the blunt-ended *Bam*HI site of the pBabe-puro vector (Morgenstern and Land, 1990). Cells were retrovirally transduced as described before (Evers et al., 1998). MDCKII cells stably transduced with the pBabe-Puro or pCMV-neo vector were selected for 4-6 days in medium containing puromycin (3 μg/ml) or for 7 days in medium containing G-418 (800 μg/ml), respectively.

Membrane preparation and immunoblotting

The virus-infected Sf9 cells were harvested, their membranes isolated and stored, and the membrane protein concentrations determined as described (Sarkadi et al., 1992). Immunoblotting, detection of human MRP1 with the R1 and M6 monoclonal antibodies, and detection of protein-antibody interactions using the enhanced chemiluminescence technique were as described previously (Bakos et al., 1996).

Tracer uptake in membrane vesicles and vanadate-dependent nucleotide trapping

[^{3}H]LTC_4 (135 Ci/mmol; DuPont NEN); [^{3}H]NEM-GS was

prepared from [^{3}H]NEM (60 Ci/mmol, DuPont NEN) by mixing the isotope with reduced glutathione (GSH) as described (Bakos et al., 1998). For [^{3}H]NEM-GS and [^{3}H]LTC$_4$ transport measurements and vanadate-dependent nucleotide trapping, see Bakos et al., 1998.

Confocal laser scanning microscopy

For immunofluorescence experiments cells were grown on microporous polycarbonate filters (3 μm pore size, 24.5 mm diameter, Transwell™ 3414; Costar Corp., Cambridge, MA, USA) at a density of 4×10^5 cells/well for 3 days. Antibody incubations with mAbs M6 and R1 were as described before (Bakos et al., 1998). Incubations with the anti-MDR1 mAb MRK16 were performed as above with the modification that cells were not permeabilized with Triton X-100. FITC-labeled secondary antibodies were from Zymed Laboratories, Inc. and from Roche diagnostics.

Transport assays with MDCKII cells

1-chloro-2,4-dinitro[^{14}C]benzene (10 Ci/mol), and [^{3}H]vinblastine (9.4 Ci/mmol) were obtained from Amersham Pharmacia Biotech. Transport experiments were carried out exactly as described (Bakos et al., 1998; Evers et al., 1998).

RESULTS

Construction and expression of chimeric MRP1-MDR1 variants

We inserted cDNAs into baculovirus and retroviral vectors to obtain the following molecules: (1) L_0 of MRP1 (aa 204-281), covalently coupled to the N terminus of MDR1 (L_0MDR1); (2) TMD_0 of MRP1 (aa 1-203), covalently coupled to the N

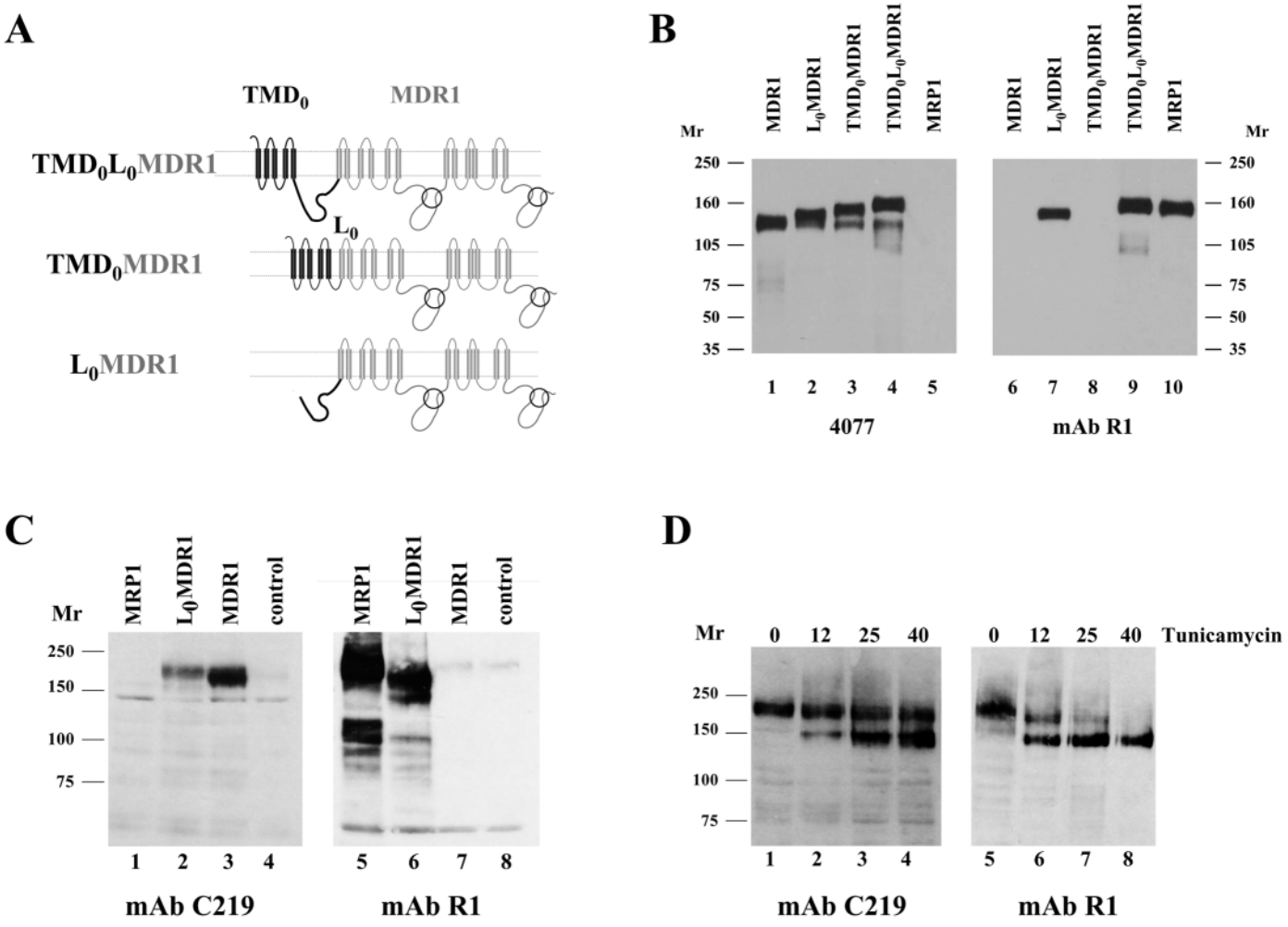

Fig. 1. Schematic representation (A) and immunoblot detection of the MRP1-MDR1 chimeric proteins expressed in Sf9 cells (B) and in MDCKII cells (C,D) by MDR1 or MRP1-specific antibodies. (A) Schematic representation of the MRP1-MDR1 chimera proteins. (B) Western blot analysis of Sf9 cell membranes containing MDR1, L_0MDR1, TMD_0MDR1, TMD_0L_0MDR1 or MRP1. Isolated membranes of Sf9 cells (5 μg) were subjected to electrophoresis in a 6% Laemmli-type gel, and immunoblotted as described in Materials and Methods. Lanes 1-5 were stained with the polyclonal antibody 4077, specific for human MDR1, while lanes 6-10 were developed with mAb R1, specific for human MRP1. Protein-antibody interactions were visualized using the enhanced chemiluminescence technique. (C) Western blot with lysates from MDCKII wild-type cells and cells producing L_0MDR1, MDR1 or MRP1. 20 μg of protein were size-fractionated in a denaturing 7.5% polyacrylamide gel. After electroblotting blots were incubated with either C219, recognising human MDR1 (lanes 1-4) or mAb R1 for human MRP1 (lanes 5-8). The identity of the cell lines is indicated over the lanes. (D) Western blots showing MDCKII-MDR1 cells (lanes 1-4) and MDCKII-L_0MDR1 cells (lanes 5-8) treated with tunicamycin (3 μg/ml) for 0, 12, 25 or 40 hours. MDR1 was visualized with mAb C219 and L_0MDR1 with mAb R1. The positions of marker proteins (M_r) are shown.

terminus of MDR1 (TMD_0MDR1); and (3) the full N-terminal region of MRP1 (TMD_0L_0, aa 1-281), covalently coupled to the N terminus of MDR1 (TMD_0L_0MDR1; see Fig. 1A). The MRP1-MDR1 chimeras were expressed in baculovirus-infected Sf9 cells and in retrovirus-infected MDCKII cells. For this latter system we only present the data for the L_0MDR1 chimera, as the role of the L_0 region is the focus of the present studies.

The protein levels and the transport properties of the various mutants were studied in intact cells and in isolated membrane preparations. Fig. 1B and C,D presents the immunoblots of the proteins detectable in membrane preparations of Sf9 cells and in retrovirally transduced MDCKII cells, respectively. The epitope for mAb R1 is within the L_0 region (aa 238-247; Hipfner et al., 1998), while those for the polyclonal Ab 4077 and mAb C219 are within MDR1 Pgp. We obtained significant expression of the chimeric MRP1-MDR1 proteins, commensurable to those of the wild-type molecules in the same expression systems. A small amount of partial proteolytic cleavage was apparent in proteins produced in the baculovirus expression system (Fig. 1B), at sites close to the artificially constructed joining regions. However, the majority of the produced proteins was found at the molecular masses corresponding to the full-length chimeras. In MDCKII cells the L_0MDR1 protein was detected at the expected molecular mass (Fig. 1C) and, like MDR1, was glycosylated; treatment of the cells with tunicamycin abolished this glycosylation (Fig. 1D).

In order to examine the functionality of the chimeric proteins, we first measured ATP-dependent LTC_4 and NEM-GS transport in isolated Sf9 cell membrane vesicles (see Bakos et al., 1998). Despite the appreciable amounts of protein detectable in the vesicles, we did not find an MRP1-like GS-conjugate transport activity exceeding that observed in the control, β-galactosidase containing membrane vesicles (Fig. 2A).

In the absence of any MRP1-like transport activity it was important to determine if the MRP1-MDR1 chimeras retained MDR1-like hydrophobic drug transport capacity. Since direct vesicular transport measurements with hydrophobic MDR1 substrates are difficult to perform, we examined the substrate-stimulated ATPase and nucleotide trapping activity of the MRP1-MDR1 chimeric proteins in isolated Sf9 membranes. Vanadate-dependent nucleotide trapping of MRP1 reflects a partial reaction of the ATPase cycle of this protein, stimulated by the transported substrates (Ueda et al., 1997). The occluded nucleotide can be visualized by covalent photoaffinity labeling, by using Mg-8-azido-[α-^{32}P]ATP.

In all membranes containing the chimeric MRP1-MDR1 proteins we found a significant verapamil-stimulated ATPase activity, characteristic for MDR1 (not shown). However, this activity may be the consequence of a partial proteolysis of the chimeras (see Fig. 1B), yielding full-length MDR1, therefore nucleotide trapping was considered more informative in this regard. Covalent photoaffinity labeling of the proteins was performed with Mg-8-azido-[α-^{32}P]ATP in the presence of vanadate as a trapping agent (see Materials and Methods). We have shown before that the MDR1 protein is capable of nucleotide trapping when stimulated by a hydrophobic compound (e.g. verapamil) and that it is not affected by LTC_4. This activity in MRP1 is significantly stimulated by LTC_4, but not by verapamil (see Bakos et al., 1998; Szabó et al., 1998).

As shown in Fig. 2B, the nucleotide trapping of the MRP1-

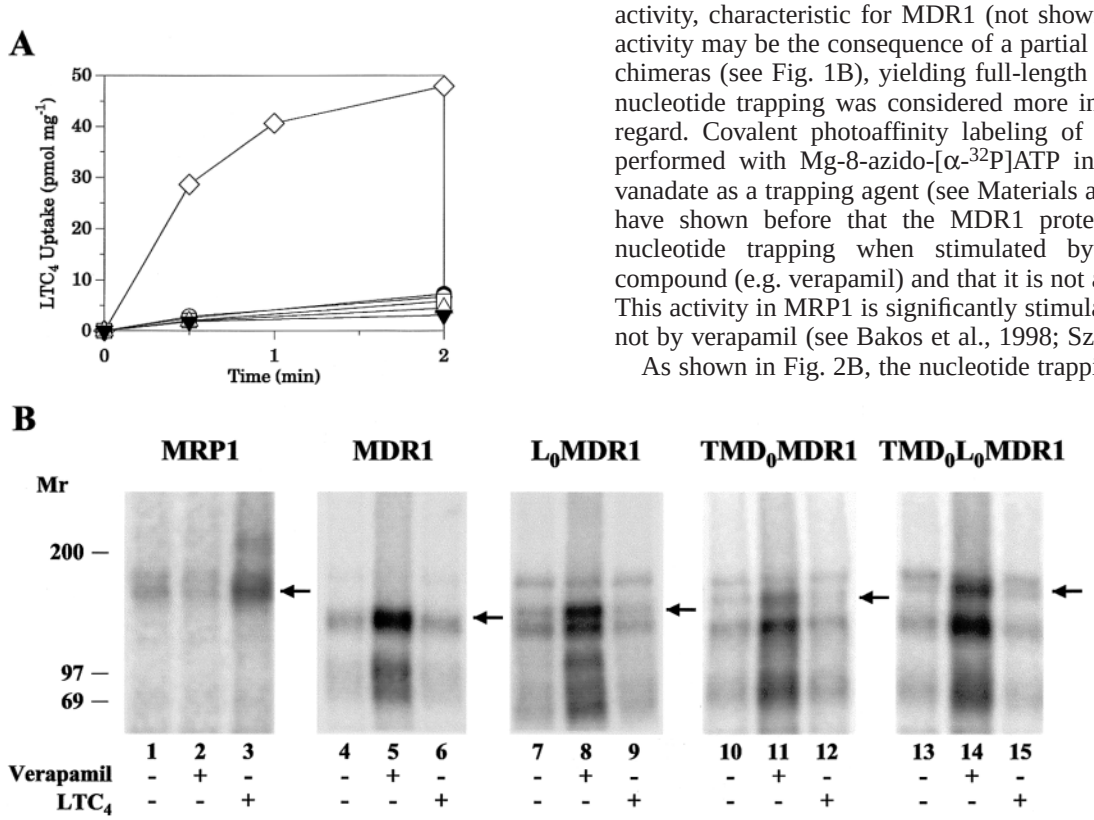

Fig. 2. LTC_4 transport (A) and nucleotide trapping (B) in Sf9 cell membranes containing MRP1-MDR1 chimeric proteins. (A) Time-course of ATP-dependent LTC_4 uptake in Sf9 membrane vesicles, expressing MRP1 (◊), MDR1 (○), TMD_0MDR1 (●), TMD_0L_0MDR1 (□), L_0MDR1 (Δ) or β-galactosidase (▼). Membrane preparations were incubated with 50 nM LTC_4 at 23°C and ATP-dependent uptake was calculated by subtracting the values obtained in the presence of 4 mM AMP from those in the presence of 4 mM ATP. Samples were taken at the time points indicated. (B) Vanadate-dependent nucleotide trapping by MRP1-MDR1 chimeric proteins. Isolated membranes from Sf9 cells (50 μg) expressing MRP1 (lanes 1-3), MDR1 (lanes 4-6), L_0MDR1 (lanes 7-9), TMD_0MDR1 (lanes 10-12) and TMD_0L_0MDR1 (lanes 13-15) were labeled with Mg-8-azido-[α-^{32}P]ATP in the presence of vanadate, as described in Materials and Methods. The reaction buffer contained 30 μM verapamil in experiments documented in lanes 2, 5, 8, 11 and 14, and 600 nM LTC_4 in lanes 3, 6, 9, 12 and 15.

MDR1 chimeras was easily measurable and was vanadate-dependent. This is in contrast to MDR1, which was not stimulated by LTC_4, but stimulated two- to fourfold in the presence of verapamil. Stimulation by verapamil was observed both in the protein bands representing the full-length MRP1-MDR1 chimeras, as well as in the proteolytic fragments representing the MDR1 core. In all cases a full inhibition of nucleotide trapping was obtained by pretreatment with 1 mM N-ethylmaleimide (data not shown). These functional assays demonstrate that the MRP1-MDR1 chimeras retained their MDR1-like nucleotide trapping function.

In the following experiments, we examined the membrane localization and transport function of the L_0MDR1 chimeric protein in retrovirally transduced MDCKII cell monolayers by CLSM. L_0MDR1 was detected using mAb MRK16, an antibody recognizing a conformational epitope on the extracellular loops of MDR1 Pgp (Hamada and Tsuruo, 1986). As shown in Fig. 3A, L_0MDR1 was predominantly localized in the apical membrane of MDCKII cell monolayers, although some cells also contained a relatively low concentration of protein in the lateral membrane. In accordance with an apical localization, the MDCKII-L_0MDR1 and MDCKII-MDR1 cells showed an increased apical transport of vinblastine (Fig. 3B). The vectorial transport activity of L_0MDR1 correlated with its protein levels as compared to that of MDR1 (Fig. 1C). We found no increased transport of the organic anion DNP-GS by the MDCKII-L_0MDR1 cells (data not shown).

The combination of these results clearly indicates that the MRP1-MDR1 chimeras were produced in both insect and mammalian cells and that the chimeric proteins retained the features of the MDR1 protein. The addition of the N-terminal MRP1 regions to MDR1 did not result in any MRP1-like transport function or a clear change in membrane localization.

Construction and expression of mutant MRP1 variants

In order to analyse the specific role of the N-terminal linker region of MRP1 in more detail, we expressed the following mutant MRP1 constructs in both Sf9 and MDCKII cells: (1) an N-terminally truncated MRP1 (aa 281-1531), containing the two ABC units and the 2× 6 TM helices (ΔMRP1; Bakos et al., 1998); (2) aa 204-281, representing the N-terminal linker region of MRP1 (L_0); (3) a deletion mutant of MRP1 lacking aa 223-232 (MRP1Δ(223-232)); (4) the L_0 region alone, but carrying the same deletion as in mutant (3) (L_0Δ(223-232)) (Fig. 4A).

Fig. 4B demonstrates the immunoblot detection of the ΔMRP1 and L_0 variants in Sf9 cells by the anti-MRP1 monoclonal antibodies R1 and M6. The epitope for mAb M6 is at the C terminus of MRP1 (aa 1511-1520; Hipfner et al., 1998). For all these molecules we obtained expression similar to that of wild-type MRP1 (Fig. 4B). It is important to note (see also below) that, like wild-type MRP1 and ΔMRP1, the L_0 polypeptide was found to be almost entirely present in the membrane fraction of the cell lysates. The amount of this membrane-bound L_0 was independent of the presence or absence of ΔMRP1 in the Sf9 cell membranes. Slight variations in the expression levels of these mutant proteins between

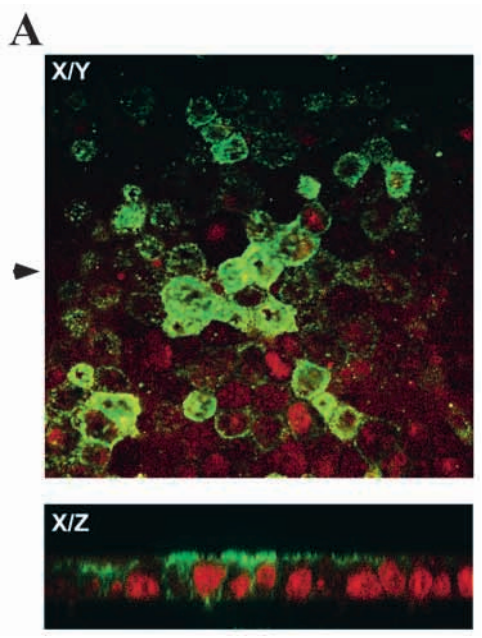

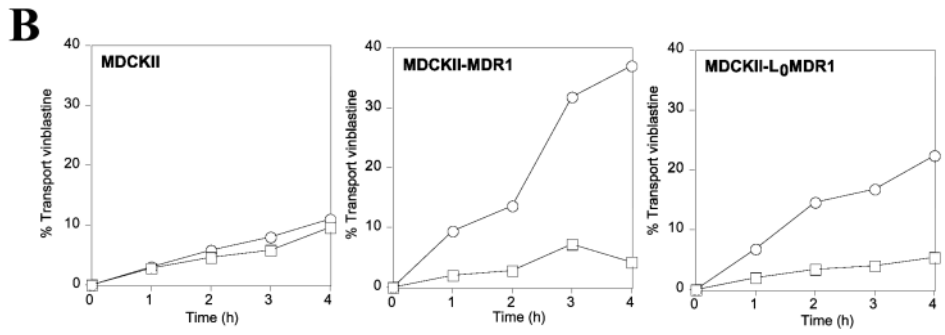

Fig. 3. Localization and transport properties of the chimera L_0MDR1 in MDCKII cells. (A) Immunolocalization of L_0MDR1 in MDCKII monolayers by confocal laser scanning microscopy. L_0MDR1 was detected by indirect immunofluorescence with mAb MRK16 (green signal). The upper part shows a top view of the monolayer, the lower part a vertical X/Z section. The arrowhead indicates the position where the section was made. Nucleic acids were counterstained with Propidium Iodide (red signal). (B) Transport of [^{3}H]vinblastine by MDCKII-derived monolayers. Transport of vinblastine by MDCKII, MDCKII-MDR1 and MDCKII-L_0MDR1 cells is shown. Transport is presented as the fraction of total radioactivity added at the beginning of the experiment (t=0), appearing in the opposite compartment. PSC833 (0.1 μM) was present in both compartments to inhibit the endogenous MDR1 Pgp present in these cells (Bakos et al., 1998). Squares, translocation from apical to basolatera; circles, translocation from basolateral to apical. The experiments were performed in duplicate and repeated twice.

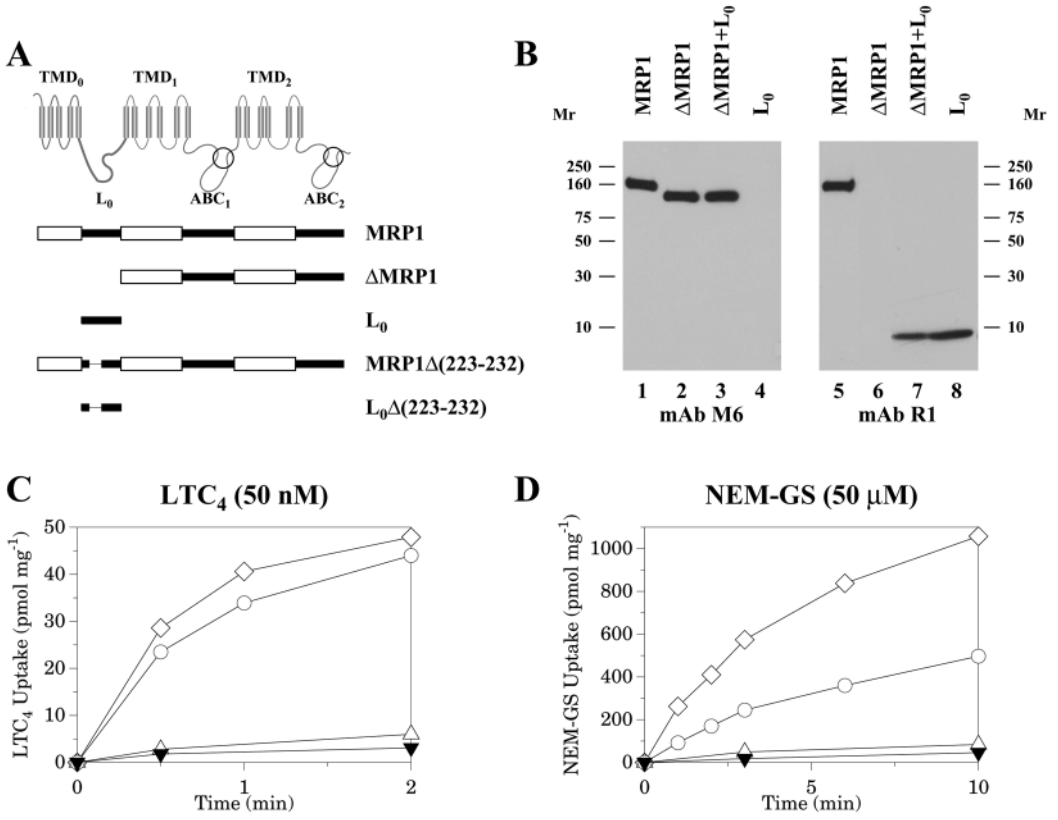

Fig. 4. Detection and function of MRP1 variants in Sf9 cell membranes. (A) Schematic representation of the MRP1 variants. (B) Western blot analysis of Sf9 cell membranes prepared from cells expressing MRP1 (lanes 1 and 5), ΔMRP1 (lanes 2 and 6), ΔMRP1 + L_0 (lanes 3 and 7) or L_0 (lanes 4 and 8). Isolated membranes of Sf9 cells (5 μg) were subjected to electrophoresis in a 4%-20% Laemmli-type gel, and immunoblotted. Blots were incubated with mAbs R1 (lanes 5-8) and M6 (lanes 1-4). (C,D) Time course of ATP-dependent LTC_4 (C) and NEM-GS (D) uptake in Sf9 cell membrane vesicles containing MRP1 (◊), ΔMRP1 (Δ), ΔMRP1+L_0 (○) or β-galactosidase (▼). (C) Membranes were incubated with 50 nM LTC_4 at 23°C; (D) Membranes were incubated with 50 μM NEM-GS at 37°C. ATP-dependent uptake was calculated by subtracting the values obtained in the presence of 4 mM AMP from those in the presence of 4 mM ATP. Samples were taken at the time points indicated.

various membrane preparations were still observed and therefore the functional data were corrected for the specific protein expression levels (see below).

In the following experiments we have examined the function of MRP1, ΔMRP1 and ΔMRP1 coexpressed with the L_0 region by measuring the transport of the established MRP1 substrates LTC_4 and NEM-GS (Bakos et al., 1998; Muller et al., 1994). In order to correctly determine the transport function of the different MRP1 proteins, we estimated the relative amount of transport-competent inside-out vesicles in the Sf9 membrane preparations (see Bakos et al., 1998), and corrected the transport rates according to the relative MRP1 expression levels, as determined by immunoblotting.

Fig. 4C,D shows the time-dependent uptake of [^{3}H]LTC_4 (50 nM) and [^{3}H]NEM-GS (50 μM) in Sf9 membrane vesicles containing MRP1, ΔMRP1, or the coexpressed L_0 and ΔMRP1. Full-length MRP1 produced an ATP-dependent increase in the vesicular radioactivity, which for LTC_4 was linear for about 30 seconds at 23°C, and for NEM-GS was linear for about 3 minutes at 37°C. The initial rate of ATP-dependent LTC_4 transport by the MRP1 containing membranes was about 60 pmol mg^{-1} min^{-1} while that of NEM-GS transport was about 250 pmol mg^{-1} min^{-1} under these conditions. As shown previously (Bakos et al., 1998), rapid washing of the vesicles with cold substrate-containing solutions did not alter the vesicular LTC_4 and NEM-GS levels, while the addition of concentrated sucrose (1 M) or low concentrations of Triton X-100 (0.02%) to the medium eliminated ATP-dependent tracer accumulation.

As demonstrated in Fig. 4C,D, we found that the expression of ΔMRP1 did not result in any transport activity (as compared to transport measured in the control, β-galactosidase containing vesicles). However, the coexpression of ΔMRP1 and the L_0 region resulted in significant uptake of LTC_4 (at 50 nM about 90% of MRP1) and NEM-GS (at 50 μM NEM-GS about 40% of MRP1). Again, in all these cases intravesicular tracer uptake was eliminated by the addition of Triton X-100 or 1 M sucrose.

Examination of the kinetic parameters for the transport of LTC_4 by the coexpressed ΔMRP1 and L_0 showed that the K_m values were similar to those of wild-type MRP1 (about 140 nM). However, for transport of NEM-GS the K_m of wild-type MRP1 was 150 μM, while that of the coexpressed ΔMRP1+L_0 was about 400 μM. The maximum transport rate in this latter case was approaching the level observed for MRP1 (data not shown).

Next, we examined substrate-stimulated, vanadate-sensitive nucleotide trapping in Sf9 cell membranes containing the

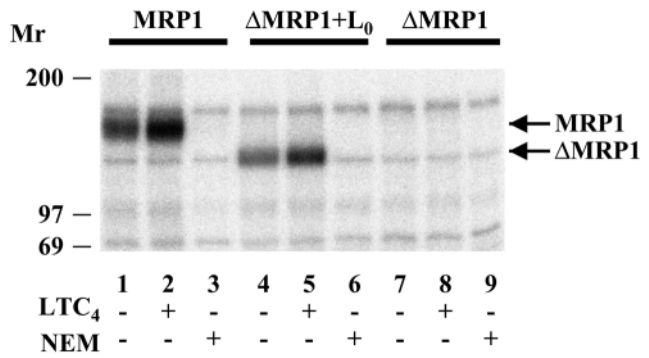

Fig. 5. Vanadate-dependent nucleotide trapping by MRP1 variants. Isolated membranes from Sf9 cells expressing MRP1 (lanes 1-3), ΔMRP1 + L_0 (lanes 4-6), or ΔMRP1 (lanes 7-9), were labeled with Mg-8-azido-[α-^{32}P]ATP in the presence of vanadate as described in Materials and Methods. The reaction buffer contained 600 nM LTC_4 (lanes 2, 5, 8), or 500 μM NEM (lanes 3, 6, 9).

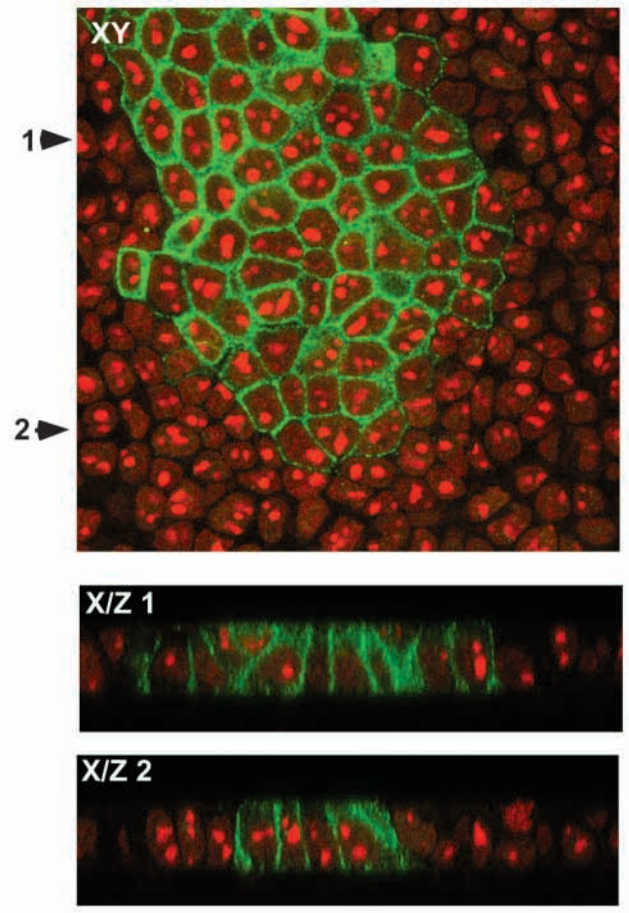

Fig. 6. Immunolocalization of L_0 coexpressed with ΔMRP1 in MDCKII monolayers by confocal laser scanning microscopy. L_0 was detected by indirect immunofluorescence with mAb R1 (green signal). The upper part shows a top view of the monolayer, the lower part a vertical X/Z section. The arrowheads indicate the positions where the sections were made. Nucleic acids were counterstained with Propidium Iodide (red signal).

various MRP1 variants (Fig. 5). As reported before (Bakos et al., 1998), ΔMRP1 did not show any nucleotide trapping. However, as shown in Fig. 5, when the L_0 region was coexpressed with the ΔMRP1 region, a full activity and stimulation of the nucleotide trapping by LTC_4 was observed, similar to that found for wild-type MRP1. Again, in all cases a full inhibition of nucleotide trapping was obtained by pretreatment with 1 mM N-ethylmaleimide (not shown).

We have shown previously that ΔMRP1 in MDCKII cells is localized in an intracellular compartment, probably the endoplasmic reticulum (Bakos et al., 1998). To investigate whether the L_0 peptide could rescue ΔMRP1 to the plasma membrane, we transduced MDCKII-ΔMRP1 cells with the pBabe-Puro-CMV-L_0 construct. Upon selection with puromycin, the localization of L_0 was determined using mAb R1. In a pool of puromycin resistant cells clear lateral plasma membrane staining was observed in small groups of cells, although some intracellular staining was also present in these cells (Fig. 6). As only a low percentage of cells showed staining with mAb R1, it was impossible to isolate single clones. Therefore, immunoblotting and transepithelial transport measurements could not be performed. No signal was obtained after infection of wild-type cells with the L_0 containing construct, probably due to rapid degradation of this small protein in the absence of ΔMRP1.

The studies documented above strongly suggest that the isolated L_0 polypeptide is able to associate with ΔMRP1 and that as a consequence the protein regains its function and routes to the lateral membrane. In the following experiments we examined the interaction of L_0 with the membrane in Sf9 cells and the possible regions within the L_0 domain that are critical for function.

As mentioned above (see Fig. 4B), a significant amount of the L_0 protein produced in Sf9 cells was found to be associated with cellular membranes. Fig. 7A documents that in the Sf9 cell lysates, most of the L_0 protein was found in the membrane fraction and only a small fraction was in the cytoplasm. Washing the Sf9 cell membranes with l M KCl did not change this membrane-bound localization of the L_0 peptide. However, washing the membranes with 5 M urea or 1% Triton X-100 completely solubilized the L_0 peptide (Fig. 7B). Coexpression of ΔMRP1 in the same cell did not affect the binding of L_0 to the membrane or sensitivity towards treatment with urea or Triton X-100. Treatment of membranes with urea had no effect on the membrane localization of MRP1 or ΔMRP1, and even treatment with 1% Triton X-100 resulted only in a 20-40% solubilization of these membrane-spanning proteins (data not shown).

The salt-insensitive, but denaturing agent- or detergent-sensitive membrane attachment of the L_0 region raised the possibility of the presence of a membrane-attaching amphipathic region (e.g. helix) within L_0. Indeed, as shown in Fig. 7C, secondary structure predictions indicated the presence of such a conserved amphipathic helix in all currently known MRP homologs (such a helix is also present in the MRP-related CFTR and SUR proteins; data not shown).

In order to examine the role of this amphipathic helix within the L_0 region, we constructed a 10-amino-acid deletion (Δ223-232) within this predicted helix, both in the context of the isolated L_0 fragment and in the full-length MRP1 molecule. Fig. 8A demonstrates that MRP1Δ(223-232) was produced in Sf9 cells in similar quantities to the wild-type MRP1 protein.

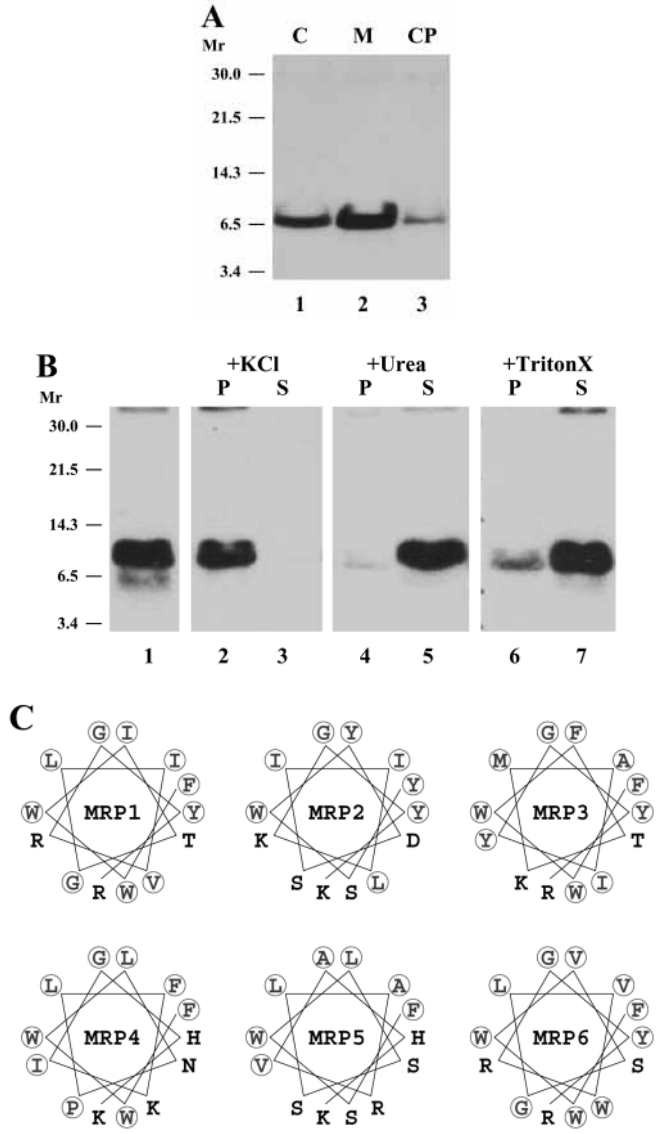

Fig. 7. Membrane attachment of the L_0 region of MRP1 expressed in Sf9 cells. (A) Detection of the L_0 region of human MRP1, expressed in Sf9 cells by western blotting. Samples were fractionated in a 20% Laemmli-type gel, immunoblotted and incubated with mAb R1. C, cell extract (5 μg); M, membrane fraction (5 μg); CP, cytoplasmic fraction, representing equivalent volumes of the cytoplasm as compared to membrane fractions. (B) Effects of KCl (1 M, lanes 2, 3), urea (5 M, lanes 4, 5), or Triton X-100 (1%, lanes 6, 7) on the membrane attachment of the L_0 region of MRP1. Membrane samples were washed with the respective agents and then size-fractionated as in A. Lane 1, isolated Sf9 cell membranes; lanes 2-7, membranes washed with the respective agents. P, membrane pellet fraction; S, supernatant fraction. Samples represent equivalent initial volumes of each fraction. (C) Computer-predicted schematic representation of an amphipathic helix within the L_0 region of various MRP proteins. Helical wheel plot of residues 221-233 in MRP1, 216-228 in MRP2, 220-232 in MRP3, 24-36 in MRP4, 112-124 in MRP5 and 216-228 in MRP6. Hydrophobic residues are circled.

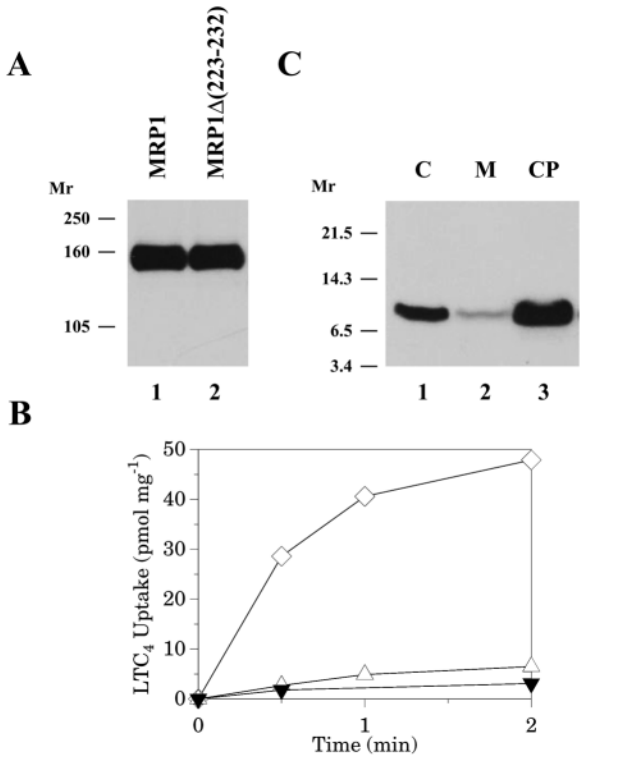

Fig. 8. Characterization of MRP1Δ(223-232) and L_0Δ(223-232) in Sf9 cells. (A) Western blot analysis of Sf9 cell membranes containing MRP1 or MRP1Δ(223-232). Isolated membranes of Sf9 cells (5 μg) were subjected to electrophoresis in a 6% Laemmli-type gel, and immunoblotted as described in Materials and Methods, with monoclonal antibody R1, specific for human MRP1. (B) Time course of ATP-dependent LTC_4 uptake in Sf9 cell membrane vesicles, expressing MRP1 (◊), MRP1Δ(223-232) (Δ) or β-galactosidase (▼). Membrane preparations were incubated with 50 nM LTC_4 at 23°C and ATP-dependent uptake was calculated by subtracting the values obtained in the presence of 4 mM AMP from those in the presence of 4 mM ATP. Samples were taken at the times indicated. (C) Detection of the L_0Δ(223-232) mutant region of human MRP1, expressed in Sf9 cells. Samples were fractionated on a 20% Laemmli-type gel, and immunoblotted by R1 antibody as described in Materials and Methods. C, cell extract (5 μg); M, membrane fraction (5 μg); CP, cytoplasmic fraction, representing an equivalent initial volume compared to the total membrane fraction.

Fig. 8B shows LTC_4 transport experiments in isolated Sf9 vesicles containing MRP1Δ(223-232). Fig. 8C shows the membrane interaction of L_0Δ(223-232). In contrast to wild-type MRP1, MRP1Δ(223-232) had no appreciable transport activity and the L_0Δ(223-232) did not attach to the cell membrane. When the L_0Δ(223-232) was coexpressed with ΔMRP1 or when a concentrated supernatant containing L_0Δ(223-232) was added to isolated ΔMRP1 containing-membranes, no transport activity for LTC_4 was observed (data not shown).

Fig. 9 shows the expression, localization and function of the MRP1Δ(223-232) protein produced in MDCKII monolayers. As shown in Fig. 9A, the MRP1Δ(223-232) protein was efficiently expressed and similar to MRP1, was almost completely glycosylated in these cells. Tunicamycin treatment resulted in the loss of glycosylation both in the MRP1 and the MRP1Δ(223-232) expressing cells (Fig. 9B). Similar to wild-type MRP1 (Bakos et al., 1998), MRP1Δ(223-232) was localized in the lateral membrane in MDCKII cells (Fig. 9C).

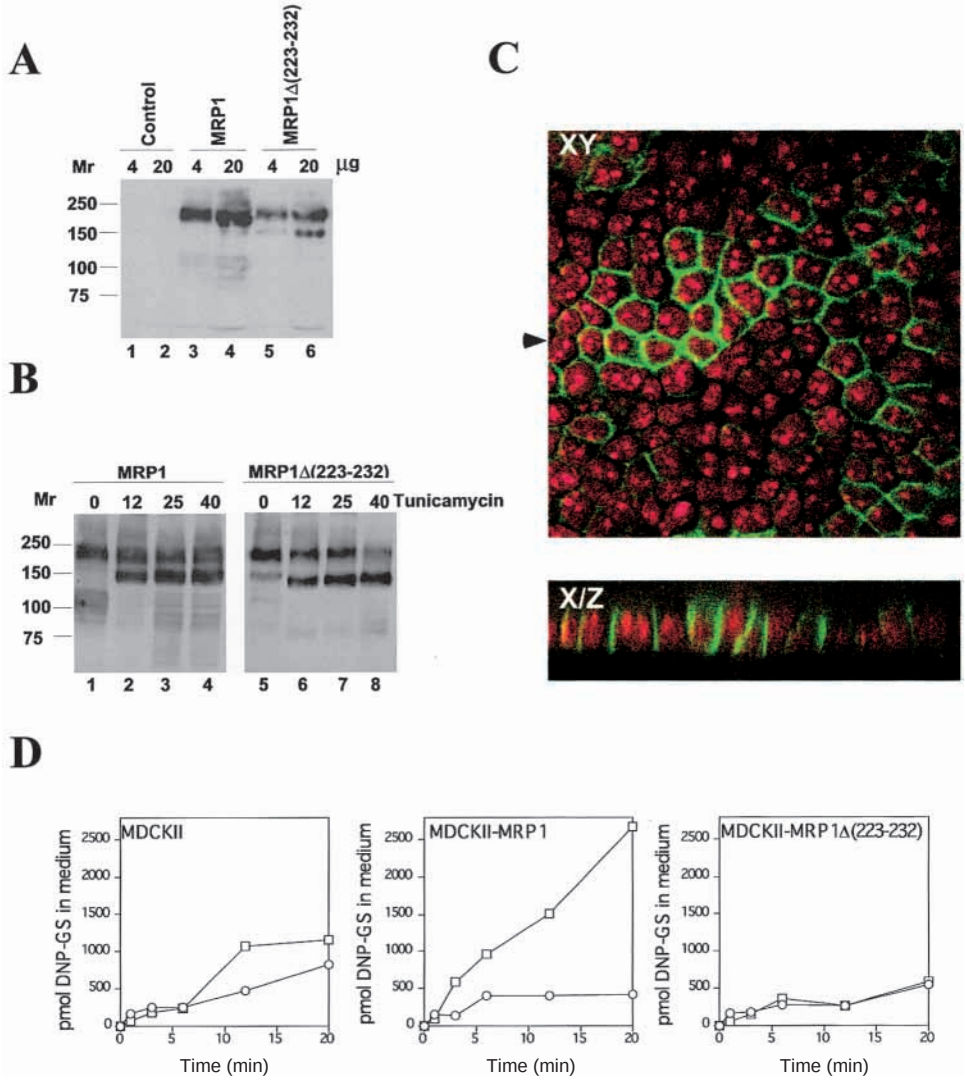

Fig. 9. Characterization of MRP1Δ(223-232) in MDCKII cells. (A) Western blot with lysates from MDCKII wild-type, MDCKII-MRP1 and MDCKII-MRP1Δ(223-232) cells. 4 or 20 μg of protein were size-fractionated. The blot was incubated with mAb R1. The identity of the cell lines is indicated over the lanes. (B) Western blot with lysates from MDCKII-MRP1 and MDCKII-MRP1Δ(223-232) cells, treated with tunicamycin (3 μg/ml) for 0, 12, 25 or 40 hours. The blots were incubated with mAb R1. (C) Immunolocalization of MRP1Δ(223-232) in MDCKII monolayers. MRP1Δ(223-232) was detected as in Fig. 6 with mAb R1. (D) Transport of DNP-GS by MDCKII derived monolayers. Cells were incubated with [^{14}C]CDNB (2 μM) in both the apical and basal compartments. This hydrophobic compound diffuses over the plasma membrane and intracellularly reacts to glutathione by the mediation of glutathione *S*-transferases. Samples were taken at 0, 1, 3, 6 and 20 minutes from both compartments and extracted with ethyl acetate to separate free CDNB from intracellularly formed DNP-GS. Squares, transport to the basolateral compartment; circles, transport to the apical compartment. The experiments were done in duplicate and repeated twice.

However, when the transport activities of MRP1 and MRP1Δ(223-232) were compared in polarised cell monolayers, there was no detectable increase in the export of DNP-GS by the MRP1Δ(223-232) protein (Fig. 9D).

DISCUSSION

We analysed the functional properties of the approximately 280-amino-acid long N-terminal region of human MRP1. The so-called TMD_0 and L_0 regions of MRP1 (see Fig. 1A) are present in several members of the MRP family, including the SUR proteins, and partially also in CFTR, but absent in the proteins of the MDR family (MDR1, MDR3 and sPGP). By fusing the N-terminal regions of MRP1 to the human MDR1 protein, and by performing various mutation and coexpression studies, we examined the role of these regions in processing, plasma membrane targeting and transport of the multidrug resistance proteins. Proteins were expressed both in Sf9 insect cells and MDCKII mammalian cells. In the first system, due to the high levels of expression in a heterologous cell type, functional studies and convenient biochemical assays could be carried out on isolated membranes with less interference from any unrelated proteins. These assays included measurements of labeled glutathione-conjugate and leukotriene C_4 transport, as well as vanadate-dependent nucleotide occlusion on isolated membrane vesicles. The polarised MDCKII cell monolayers offered the possibility to efficiently study membrane routing and transcellular transport properties of the overproduced proteins.

In order to study the role of the N-terminal regions of MRP1, we constructed chimeric MRP1-MDR1 proteins, in which MDR1 was extended either with the full-length N-terminal region of MRP1 (TMD_0+L_0), or with the two separate subcomponents (TMD_0 or L_0) of this region. We found that all of these proteins were properly expressed in both the Sf9 and MDCKII cells, and essentially preserved the transport, nucleotide occlusion and apical membrane routing features of the wild-type MDR1. Most likely the MDR1 protein could not be converted to MRP1 by these manipulations, as specific interdomain interactions are required for the function of this region within MRP1 (see below). It is interesting to note, however, that these N-terminally extended MDR1 proteins were properly folded and inserted into the membrane to retain their transport function. Although we detected some lateral staining of the L_0MDR1 molecule in MDCKII cells (Fig. 3A),

this was probably not due to the presence of a dominant lateral routing signal in L_0 as we observed the same in cells producing TMD_0MDR1 (data not shown). We therefore consider it more likely that the apical routing signal present in MDR1 was partially masked in these chimeric proteins.

As documented in our earlier studies (Bakos et al., 1998), the N-terminally truncated MRP1 core (ΔMRP1) could be expressed in Sf9 and mammalian cells, but was non-functional. Our previous studies also indicated that a truncated MRP1, containing a covalently attached L_0 but no TMD_0 region, resulted in a functional MRP1-like protein that was correctly routed to the plasma membrane (Bakos et al., 1998). Here we document that when the non-functional MRP1 core was coexpressed with the isolated L_0 molecule in Sf9 cells a functional MRP1 protein was obtained, with essentially the same transport and nucleotide-trapping characteristics as the wild-type protein. Thus a covalent linkage between the MRP1 core and the L_0 region is not required. As noted for the L_0MRP1 construct in our previous experiments (Bakos et al., 1998), the coexpressed L_0+ΔMRP1 had a higher K_m for GS-conjugates than the wild-type MRP1, and thus some regulatory role of the TMD_0 region may be absent in these proteins.

When ΔMRP1 was coexpressed with the L_0 region in polarised MDCKII cells, we found that L_0 was routed to the lateral membrane (Fig. 6), most likely together with ΔMRP1. Similar results were obtained in coexpression experiments with the TMD_0L_0 region, in which we could show a partial relocalization of ΔMRP1 and TMD_0L_0 to the plasma membrane (data not shown). Although in MDCKII cells, for technical reasons, transport by these coproduced proteins could not be measured, these results suggest that the isolated TMD_0L_0 and L_0 peptides can properly fold, attach to the cell membrane and associate with ΔMRP1. All coexpression studies in Sf9 and MDCKII cells indicate that the L_0 region is a distinct protein domain within the MRP1 protein that works in specific association with the core region of MRP1.

It is possible that the L_0 region contains a routing signal sufficient to induce lateral routing of the ΔMRP1 fragment. However, we cannot exclude that ΔMRP1 alone is not properly folded in MDCKII cells and therefore gets stuck in the endoplasmic reticulum. Association with L_0 may result in proper folding and transport to the plasma membrane. Experiments are in progress to discriminate between these possibilities.

In the experiments with Sf9 membranes we found that the isolated L_0 peptide, which was predicted to be localized in the cytoplasm, was attached to membranes and could be solubilized only by treatment with urea or detergents. This membrane interaction of L_0 did not require the presence of the ΔMRP1 protein. Computer-based secondary structure predictions indicated that the L_0 region has two alpha-helical regions, one of which (aa 221-233) is a characteristic amphipathic helix, conserved in all members of the MRP family (Fig. 7C). Such an amphipathic helix may produce hydrophobic interactions with the lipid phase of the cell membrane or with hydrophobic regions of other membrane proteins.

In order to analyse the role of the predicted amphipathic alpha-helical region within L_0, a mutant was generated in which this region was deleted. When MRP1Δ(223-232) was expressed in both Sf9 and MDCKII cells, we found that this deletion eliminated MRP1 transport function, but did not affect glycosylation or membrane routing. Moreover, when the isolated L_0Δ(223-232) was produced in Sf9 cells, the mutation abolished the hydrophobic membrane attachment of the L_0 region and eliminated any functional re-activation of the ΔMRP1 construct. These experiments suggest that the hydrophobic alpha-helix within the L_0 region participates in membrane attachment and is absolutely required for the function of MRP1.

As MRP1 may play a major role in clinical chemotherapy resistance of human tumors (Hipfner et al., 1999), information regarding its key functional domains and the identification of small specific peptide regions should significantly help in the design of efficient inhibitors for this drug pump. Further investigation of the structural and functional features of the L_0 domain should promote this work, with the possibility of devising agents serving clinical applications.

This work has been supported by research grants from COST, OMFB, OTKA (Grants D32847, T022072, T029921), FKFP and ETT, Hungary, and by the Deutsche Forschungsgemeinschaft (Grant EV39-I-I to R.E.). B. Sarkadi is a recipient of a Howard Hughes International Scholarship. We thank Dr Piet Borst for advice and critical reading of the manuscript. We also thank Drs Matthias Kneussel and Heinrich Betz (Max-Planck-Institute for Brain Research, Frankfurt) for giving us the opportunity to use their CLSM facility, and Drs Rik Scheper, Marcel Flens and Henk Broxterman (Free University Hospital, Amsterdam) for providing the anti-MRP1 and MRK16 monoclonal antibodies, respectively. Technical help by Ilona Zombori, Györgyi Demeter and Sara Mateus Fernández is gratefully acknowledged.

REFERENCES

Bakos, É., Evers, R., Sinkó, E., Váradi, A., Borst, P. and Sarkadi, B. (2000). Interactions of the human multidrug resistance proteins MRP1 and MRP2 with organic anions. *Mol. Pharmacol.* **57**, 760-768.

Bakos, É., Evers, R., Szakács, G., Tusnády, G. E., Welker, E., Szabó, K., de Haas, M., van Deemter, L., Borst, P., Váradi, A. et al. (1998). Functional multidrug resistance protein (MRP1) lacking the N-terminal transmembrane domain. *J. Biol. Chem.* **273**, 32167-321675.

Bakos, É., Hegedüs, T., Holló, Z., Welker, E., Tusnády, G. E., Zaman, G. J., Flens, M. J., Váradi, A. and Sarkadi, B. (1996). Membrane topology and glycosylation of the human multidrug resistance-associated protein. *J. Biol. Chem.* **271**, 12322-12326.

Chang, X. B., Hou, Y. X. and Riordan, J. R. (1998). Stimulation of ATPase activity of purified multidrug resistance-associated protein by nucleoside diphosphates. *J. Biol. Chem.* **273**, 23844-23848.

Doyle, L. A., Yang, W., Abruzzo, L. V., Krogmann, T., Gao, Y., Rishi, A. K. and Ross, D. D. (1998). A multidrug resistance transporter from human MCF-7 breast cancer cells [published erratum appears in Proc. Natl. Acad. Sci. USA 1999 Mar 2;96(5):2569]. *Proc. Natl. Acad. Sci. USA* **95**, 15665-156670.

Evers, R., de Haas, M., Sparidans, R., Beijnen, J., Wielinga, P. R., Lankelma, J. and Borst, P. (2000). Vinblastine and sulfinpyrazone export by the multidrug resistance protein MRP2 is associated with glutathione export. *Br. J. Cancer* **83**, 375-383.

Evers, R., Kool, M., van Deemter, L., Janssen, H., Calafat, J., Oomen, L. C., Paulusma, C. C., Oude Elferink, R. P., Baas, F., Schinkel, A. H. et al. (1998). Drug export activity of the human canalicular multispecific organic anion transporter in polarized kidney MDCK cells expressing cMOAT (MRP2) cDNA. *J. Clin. Invest.* **101**, 1310-1319.

Evers, R., Zaman, G. J., van Deemter, L., Jansen, H., Calafat, J., Oomen, L. C., Oude Elferink, R. P., Borst, P. and Schinkel, A. H. (1996). Basolateral localization and export activity of the human multidrug resistance-associated protein in polarized pig kidney cells. *J. Clin. Invest.* **97**, 1211-1218.

Gao, M., Yamazaki, M., Loe, D. W., Westlake, C. J., Grant, C. E., Cole, S. P. and Deeley, R. G. (1998). Multidrug resistance protein. Identification

of regions required for active transport of leukotriene C4. *J. Biol. Chem.* **273**, 10733-10740.

Gottesman, M. M. and Pastan, I. (1993). Biochemistry of multidrug resistance mediated by the multidrug transporter. *Annu. Rev. Biochem.* **62**, 385-427.

Hamada, H. and Tsuruo, T. (1986). Functional role for the 170- to 180-kDa glycoprotein specific to drug-resistant tumor cells as revealed by monoclonal antibodies. *Proc. Natl. Acad. Sci. USA* **83**, 7785-7789.

Hipfner, D. R., Deeley, R. G. and Cole, S. P. (1999). Structural, mechanistic and clinical aspects of MRP1. *Biochim. Biophys. Acta* **1461**, 359-376.

Hipfner, D. R., Gao, M., Scheffer, G., Scheper, R. J., Deeley, R. G. and Cole, S. P. (1998). Epitope mapping of monoclonal antibodies specific for the 190-kDa multidrug resistance protein (MRP). *Br. J. Cancer* **78**, 1134-1140.

Jedlitschky, G., Leier, I., Buchholz, U., Barnouin, K., Kurz, G. and Keppler, D. (1996). Transport of glutathione, glucuronate, and sulfate conjugates by the MRP gene-encoded conjugate export pump. *Cancer Res.* **56**, 988-994.

Jedlitschky, G., Leier, I., Buchholz, U., Center, M. and Keppler, D. (1994). ATP-dependent transport of glutathione S-conjugates by the multidrug resistance-associated protein. *Cancer Res.* **54**, 4833-4836.

Loe, D. W., Almquist, K. C., Cole, S. P. and Deeley, R. G. (1996a). ATP-dependent 17 beta-estradiol 17-(beta-D-glucuronide) transport by multidrug resistance protein (MRP). Inhibition by cholestatic steroids. *J. Biol. Chem.* **271**, 9683-9689.

Loe, D. W., Almquist, K. C., Deeley, R. G. and Cole, S. P. (1996b). Multidrug resistance protein (MRP)-mediated transport of leukotriene C4 and chemotherapeutic agents in membrane vesicles. Demonstration of glutathione-dependent vincristine transport. *J. Biol. Chem.* **271**, 9675-9682.

Loe, D. W., Deeley, R. G. and Cole, S. P. (1998). Characterization of vincristine transport by the M(r) 190,000 multidrug resistance protein (MRP): evidence for cotransport with reduced glutathione. *Cancer Res.* **58**, 5130-5136.

Mao, Q., Leslie, E. M., Deeley, R. G. and Cole, S. P. (1999). ATPase activity of purified and reconstituted multidrug resistance protein MRP1 from drug-selected H69AR cells. *Biochim. Biophys. Acta* **1461**, 69-82.

McGrath, T., Latoud, C., Arnold, S. T., Safa, A. R., Felsted, R. L. and Center, M. S. (1989). Mechanisms of multidrug resistance in HL60 cells. Analysis of resistance associated membrane proteins and levels of mdr gene expression. *Biochem. Pharmacol.* **38**, 3611-3619.

Morgenstern, J. P. and Land, H. (1990). Advanced mammalian gene transfer: high titre retroviral vectors with multiple drug selection markers and a complementary helper-free packaging cell line. *Nucleic Acids Res.* **18**, 3587-3596.

Muller, M., Meijer, C., Zaman, G. J., Borst, P., Scheper, R. J., Mulder, N. H., de Vries, E. G. and Jansen, P. L. (1994). Overexpression of the gene encoding the multidrug resistance-associated protein results in increased ATP-dependent glutathione S-conjugate transport. *Proc. Natl. Acad. Sci. USA* **91**, 13033-13037.

Sarkadi, B., Price, E. M., Boucher, R. C., Germann, U. A. and Scarborough, G. A. (1992). Expression of the human multidrug resistance cDNA in insect cells generates a high activity drug-stimulated membrane ATPase. *J. Biol. Chem.* **267**, 4854-4858.

Scarborough, G. A. (1995). Drug-stimulated ATPase activity of the human P-glycoprotein. *J. Bioenerg. Biomembr.* **27**, 37-41.

Szabó, K., Welker, E., Bakos, É., Muller, M., Roninson, I., Váradi, A. and Sarkadi, B. (1998). Drug-stimulated nucleotide trapping in the human multidrug transporter MDR1. Cooperation of the nucleotide binding domains. *J. Biol. Chem.* **273**, 10132-10138.

Taguchi, Y., Yoshida, A., Takada, Y., Komano, T. and Ueda, K. (1997). Anti-cancer drugs and glutathione stimulate vanadate-induced trapping of nucleotide in multidrug resistance-associated protein (MRP). *FEBS Lett.* **401**, 11-14.

Tusnády, G. E., Bakos, É., Váradi, A. and Sarkadi, B. (1997). Membrane topology distinguishes a subfamily of the ATP-binding cassette (ABC) transporters. *FEBS Lett.* **402**, 1-3.

Ueda, K., Inagaki, N. and Seino, S. (1997). MgADP antagonism to Mg^{2+}-independent ATP binding of the sulfonylurea receptor SUR1. *J. Biol. Chem.* **272**, 22983-22986.

Zaman, G. J., Flens, M. J., van Leusden, M. R., de Haas, M., Mulder, H. S., Lankelma, J., Pinedo, H. M., Scheper, R. J., Baas, F., Broxterman, H. J. et al. (1994). The human multidrug resistance-associated protein MRP is a plasma membrane drug-efflux pump. *Proc. Natl. Acad. Sci. USA* **91**, 8822-8826.